Astronomy & Astrophysics manuscript no. output
March 4, 2023

Dating young open clusters using δ Scuti stars

Results for Trumpler 10 and Praesepe

D. Pamos Ortega, G. M. Mirouh, A. García Hernández, J. C. Suárez Yanes, and S. Barceló Forteza

Departamento de Física Teórica y del Cosmos, Universidad de Granada, Campus de Fuentenueva s/n, 18071, Granada, Spain
e-mail: davidpamos@correo.ugr.es

ABSTRACT

Aims. The main goal of this work is to date young open clusters using δ Sct stars. Seismic indices as the large separation and the frequency at maximum power can help to constrain the models in order to better characterize the stars. We add a reliable method to identify some radial modes, which gives us greater confidence in the constrained models.
Methods. We extract the frequency content of a δ Sct stars sample belonging to the same open cluster. We estimate the low-order large separation by different techniques, and the frequency at maximum power for each member of the sample. We use a grid of models built with the typical parameters of δ Sct stars, including these seismic indices. We select the observed frequencies whose ratios that match those of the models. Once we find a range of radial modes matching the observed frequencies, mainly the fundamental mode, we add the frequency ratios to the other seismic parameters to better constrain the stellar age. Assuming star groups have similar chemistry and age, we estimate their mean age by applying a Kernel Density Estimation (KDE) fit to the age distribution of the seismically constrained models.
Results. We estimate the seismic ages of Trumpler 10, with a mean age of 19 ± 22 Myr, and Praesepe, with a mean age of 780 ± 290 Myr. In this latter case, we find two apparent populations of δ Sct stars in the same cluster, one at 590 ± 210 Myr and another at 870 ± 210 Myr. This may be due to the different rotational velocities of the members in our sample of stars, as a rapid rotation may modify the observed large separation.

Key words. Physical data and processes: asteroseismology – Stars: variables: delta Scuti – The Galaxy: open clusters and associations: general

1. Introduction

Determining the age of a star is essential to know its internal physics. Regarding the dating a star cluster, the importance lies in understanding the structure and evolution of the galaxy. However, age is not a direct observable, inferring it accurately is not an easy task. In addition, the ambiguity is made larger since we cannot be sure that all the stars in the cluster formed at the same epoch. Recent works have shown that different populations, or generations, of stars may coexist within the same cluster (e.g. Bastian & Lardo 2018). For instance, Costa et al. (2019) find two distinct populations of 176 Myr and 288 Myr stars in NGC 1866, combining an analysis of its best-studied Cepheids with that of a very accurate colour-magnitude diagram (CMD) obtained from the Hubble Space Telescope photometry. Nonetheless, Krause et al. (2020) show we can still assume one population, after which clusters remain essentially clear of gas by cluster winds.

Traditionally, isochrone fitting on the Hertzsprung-Russell diagram (HRD) has been used to date clusters. This method works when dealing with old globular clusters, where we can find a large sample of stars leaving the main sequence and evolving past the turn-off point. However, the ambiguity of this method is greater with young clusters, with a majority of stars still on the main sequence (MS). The method based on spectroscopic observations of lithium (Basri & Martín 1999; Stauffer et al. 1999) also generates large ambiguities because of unresolved binary stars (Martín et al. 2001). The relation between the rotation rate and the age of late F to M stars, called gyrochronology (Barnes 2003), seems to provide a method with which to reduce the uncertainty on the age of evolved clusters. Other methods based on chemical clocks (da Silva et al. 2012; Spina et al. 2017; Moya et al. 2022) seem to help reduce the uncertainties, making use of machine learning techniques. The drawback is that these algorithms are trained with models of highly evolved stars, for which it has been possible to obtain reliable spectroscopic observations. Therefore, despite the progress achieved with these new techniques, we still do not have a reliable method to date young open clusters, the goal of our research.

In Pamos Ortega et al. (2022) (DPO22 from now on), we proposed the use of seismic parameters to date a group of eleven δ Sct stars belonging to the young open cluster α *Per*. One of these seismic indices is the large separation, defined as the difference between acoustic modes of the same degree and consecutive radial orders, related to the mean density and the surface gravity of the star. This regularity in the frequency pattern is also present in the low-order regime ($n = [2, 8]$) (Suárez et al. 2014; García Hernández et al. 2015, 2017; Mirouh et al. 2019), where δ Sct stars show their oscillation modes. Another parameter is the frequency at maximum power, directly related to the effective temperature, used in solar-type stars and found in δ Sct stars as well (Barceló Forteza et al. 2018, 2020; Bowman & Kurtz 2018; Hasanzadeh et al. 2021).

In this work, we date the young open clusters Trumpler 10 and Praesepe, using a corresponding sample of δ Sct stars. We use only seismic parameters, such as the low-order large sepa-

ration and the frequency at maximum power, and include key information from radial modes by means of the frequency ratios. These clusters are of very different ages, which allows us to better understand the possibilities of the method.

The structure of the paper is as follows: in Sect. 2, we provide the estimated ages of the clusters Trumpler 10 and Praesepe from previous works. In Sect. 3, we introduce the sample of δ Sct stars used in this research. In Sect. 4, we present how their seismic parameters have been computed. In Sect. 5, we describe the details of the grids of models built to characterize our δ Sct stars. In Sect. 6, we explain the method to estimate a range for the fundamental mode and radial overtones in the frequency content of the analysed star. In Sect. 7, we present the ages we estimate and discuss their reliability by comparing them with the observed parameters and the literature. And finally, in Sect. 8, we lay out the main conclusions of our research and leads to improve our method.

2. The ages of Trumpler 10 and Praesepe in the literature

Trumpler 10 and Praesepe have been dated through many different techniques. Table 1 summarizes the ages and metallicities derived in the last twenty years.

Trumpler 10 (C 0846-423) is an open cluster located in the Vela constellation. According to the Milky Way Star Clusters (MWSC) catalog (Kharchenko et al. 2013), it is at a distance of about 417 pc from the Sun and has an age of log(age) = 7.380 ($\approx$ 34 Myr). According to Netopil et al. (2016), it has an age of 40±10 Myr, with a metallicity of [Fe/H] = −0.12±0.06, obtained from various photometric systems and calibrations. The work of Dias et al. (2021) computes the age for this cluster in log(age) = 7.753±0.026 ($\approx$ 57 Myr), with a metallicity of [Fe/H] = 0.043± 0.050. For these estimates, they used Gaia DR2 photometry and a grid of Padova isochrones. According to all these references, the age of Trumpler 10 lies between 34 Myr and 57 Myr.

Praesepe (M44, NGC2632) is an open cluster located in the Cancer constellation. Being one of the closest clusters to the Sun, it is also one of the most studied (see for example Suárez et al. 2002; Meibom & Mathieu 2005; Fossati et al. 2008; Brandt & Huang 2015; Choi et al. 2016; Cummings et al. 2017; Gaia Collaboration et al. 2018, and references therein). Also taking as reference the MWSC survey, it is at a distance of about 187 pc and has an age of log(age) = 8.920 ($\approx$ 729 Myr). According to Netopil et al. (2016), it has an age of 730±190 Myr and a metallicity of [Fe/H] = 0.13 ± 0.03, also obtained from different photometric systems, as for Trumpler 10. The work of Dias et al. (2021) yields log(age) = 8.882 ± 0.035 ($\approx$ 762 Myr), with a metallicity of [Fe/H] = 0.196 ± 0.039. Zhong et al. (2020) estimate the metallicity at [Fe/H] = 0.22 ± 0.08, using Large Sky Area Multi-Object Fibre Spectroscopy Telescope (LAMOST) spectroscopy. Meibom & Mathieu (2005) provides an age estimate for Praesepe of about 630 Myr. They used a completely different technique, by looking at the circularization of binary systems of solar-like stars: this circularization happens over time, so systems become circular at higher and higher separations, so that the measurement of the period of circular systems yields an age value. Douglas et al. (2019) estimate an age of 670±67 Myr. Actually, they computed the age of the open cluster Hyades, using a gyrochronology model tuned with slow rotators in Praesepe and the Sun, assuming that the two clusters are coeval, based on the similarity of their CMDs, activity, rotation and lithium abundance. In short, all these references of the last twenty years provide ages for Praesepe between 590 and 790 Myr.

3. The data

Firstly, we cross-match the VizieR Online Data Catalogue Gaia DR2 of open cluster members (Cantat-Gaudin et al. 2018) and the TESS Input Catalogue (TIC Stassun 2019), searching possible δ Sct stars belonging to the same open cluster.

According to the definition of a pure δ Sct from Grigahcène et al. (2010) and Uytterhoeven et al. (2011), we find a list of 5 candidates in the field of Trumpler 10 (Table 2) and a list of 6 candidates in the field of Praesepe (Table 3). For our Praesepe stars, we find values for the projected rotational velocity $v \sin i$, the metallicity and the spectral type, consulting the available references in Simbad Astronomy Database[1]. For the Trumpler 10 stars, only data about the spectral type is available. These parameters are useful in our discussion of the results in Sect. 7.

We perform a frequency analysis using data from sector 35 of the *TESS* mission (Ricker et al. 2014) for the Trumpler 10 sample, with approximately 13800 points; and from sector 45 for Praesepe, with approximately 15500 points. In both cases, the Rayleigh resolution is approximately 0.041 d^{-1} and the cadence around two minutes. We use the Pre-Search Data Conditioned (PDC) light curves, corrected for instrumental effects, that are publicly available through the TESS Asteroseismic Science Consortium (TASC)[2].

Using MultiModes[3], we extract the frequency content of each star in our sample. It is a python code that calculates the Fast Lomb-Scargle periodogram (Press & Rybicki 1989) of a light curve. It extracts, one by one, a limited number of significant signals, and uses their corresponding parameters (amplitudes, frequencies) to fit the total signal to a multisine function with a non-linear least squares minimization. We adopt a signal to noise ratio $SNR > 4.0$ as a stop criterion (Breger et al. 1993), to avoid spurious frequencies, and we filter possible frequency combinations. The code is presented in detail in DPO22 and in the public repository.

Fig. 1 and Fig. 2 show, respectively, the extracted frequency spectrum of each δ Sct candidate in Trumpler 10 and Praesepe. The values of the ten highest amplitudes frequencies for each star in both clusters are shown in Table A.1. The whole table with all the extracted frequencies are only available on-line.

4. Seismic parameters

Sometimes it is possible to find regularities in the complex frequency pattern of a δ Sct star (García Hernández et al. 2009; Paparó et al. 2016; Bedding et al. 2020). Following the same techniques as in García Hernández et al. (2009, 2013); Ramón-Ballesta et al. (2021) and used in DPO22, we estimate the large separation in the low order regime, $\Delta\nu_{low}$. Fig. 3 shows an example of this, where we use the Discrete Fourier Transform (DFT), the Autocorrelation Diagram (AC) applied on the frequencies, the Frequency Difference Histogram (FDH) and the échelle diagram (ED), in order to find regularities in the frequency content of TIC 28943819 (see Appendix B for the rest of our sample). The theoretical works of García Hernández et al. (2009); Reese et al. (2017) use the AC and the FT to search for the low-order large separation. They point out that its half value may be visible in the DFT, as it is the case here. We estimate the uncertainties using the width of the peaks in the DFT or the AC, depending on the case. Of all the stars analyzed in this way, TIC 28944596

[1] https://simbad.unistra.fr/simbad/
[2] https://tasoc.dk
[3] https://github.com/davidpamos/MultiModes

Table 1: The ages and metallicities for Trumpler 10 and Praesepe, in some of the main references of the last twenty years, used in this work. They used very different techniques, such as photometry, isochrones, spectroscopy, gyrochronology or circularization of binary systems

Reference	Age Trumpler 10 (Myr)	Age Praesepe (Myr)	Z Trumpler 10	Z Praesepe
Meibom & Mathieu (2005)	-	630	-	-
Fossati et al. (2008)	-	590^{+150}_{-120}	-	0.024 ± 0.002
Kharchenko et al. (2013)	34	729	-	0.025 ± 0.002
Netopil et al. (2016)	40 ± 10	730 ± 190	0.014 ± 0.002	0.024 ± 0.002
Douglas et al. (2019)	-	670 ± 67	-	-
Zhong et al. (2020)	-	-	-	0.031 ± 0.005
Dias et al. (2021)	57	762	0.018 ± 0.004	0.028 ± 0.002

Table 2: Stellar parameters of the selected targets in Trumpler 10. From left to right: mass, radii, density, surface gravity, effective temperature, cluster member probability and spectral type. References: [1]Stassun (2019), [2]Cantat-Gaudin et al. (2018), [3]Skiff (2014)

TIC	$M(M_\odot)^1$	$R(R_\odot)^1$	$\bar{\rho}(\bar{\rho}_\odot)$	$logg^1$	$\tilde{T}^{\rm eff}(K)^1$	P^2_{member}	Spectral type[3]
28943819	2.2 ± 0.3	1.60 ± 0.06	0.53 ± 0.14	4.37 ± 0.08	8646 ± 161	1.0	-
30307085	2.5 ± 0.3	1.47 ± 0.04	0.80 ± 0.17	4.51 ± 0.06	9931 ± 202	0.8	A0
28944596	2.1 ± 0.3	1.72 ± 0.06	0.41 ± 0.10	4.28 ± 0.07	8383 ± 149	1.0	A2
271061334	2.2 ± 0.3	1.58 ± 0.05	0.56 ± 0.13	4.38 ± 0.07	8773 ± 170	0.9	-
271062192	2.2 ± 0.3	1.68 ± 0.05	0.46 ± 0.11	4.33 ± 0.07	8689 ± 158	1.0	A3

Table 3: Stellar parameters of the selected targets in Praesepe. From left to right: mass, radii, density, surface gravity, effective temperature, cluster member probability, projected rotational velocity, metallicity and spectral type. References: [1]Stassun (2019), [2]Cantat-Gaudin et al. (2018), [3]Cummings et al. (2018), [4]Fossati et al. (2008), [5]Bochanski et al. (2018)

TIC	$M(M_\odot)^1$	$R(R_\odot)^1$	$\bar{\rho}(\bar{\rho}_\odot)$	$logg^1$	$\tilde{T}^{\rm eff}(K)^1$	P^2_{member}	v sini (km/s)	[Fe/H][4]	[Fe/H][5]	Spectral type[4]
175194881	1.9 ± 0.3	2.10 ± 0.07	0.20 ± 0.05	4.07 ± 0.08	7873 ± 125	1.0	85[4]	0,26	-	A7V
175264376	1.7 ± 0.3	2.13 ± 0.09	0.17 ± 0.05	4.01 ± 0.08	7416 ± 141	1.0	200[4]	0,12	0,08	F0Vn
175265807	1.9 ± 0.3	1.92 ± 0.06	0.26 ± 0.07	4.14 ± 0.08	7826 ± 126	1.0	135[3]	-	0,01	-
175291778	1.9 ± 0.3	2.31 ± 0.06	0.15 ± 0.04	3.98 ± 0.08	7865 ± 126	1.0	150[4]	0,09	-0,08	A7V
184914505	1.7 ± 0.3	1.94 ± 0.06	0.23 ± 0.06	4.09 ± 0.08	7369 ± 108	1.0	90[4]	0,31	-	A5
184917633	1.7 ± 0.3	2.08 ± 0.07	0.19 ± 0.05	4.03 ± 0.08	7443 ± 122	1.0	155[4]	-0,02	-0,02	A5

and TIC 271062192 are the most difficult cases. TIC 28944596 (see Fig. B.2) has a small number of frequencies. Its DFT shows a peak around 20 μHz and another around 40 μHz. It also shows one around 80 μHz. The AC also shows two peaks very close to 80 μHz, and the FDH shows three peaks between 70 and 80 μHz. For all this reasons, the large separation has been estimated around 80 μHz for this star. TIC 271062192 (Fig. B.4) has been an even more complicated case, because the AC, the FDH and the ED do not show regularities in the frequency content. The only evidence we have here is the DFT to estimate the large separation. It shows three congruent peaks around 19, 38 and 76 μHz. That is why we have estimated their large separation around 76 μHz.

We also compute the frequency at maximum power, following the method of Barceló Forteza et al. (2020), who use a relation between $\nu_{\rm max}$ and a theoretical or seismic effective temperature, $\tilde{T}^{\rm eff}$, obtained with a sample of pure δ Sct stars. As in this work, we have taken $\nu_{\rm max}$ as the average frequency weighted over the amplitudes A_i of the frequencies ν_i of the envelope:

$$\nu_{max} = \frac{\sum A_i \cdot \nu_i}{\sum A_i} \quad (1)$$

Following Barceló Forteza et al. (2020), we relate ν_{max} and $\tilde{T}^{\rm eff}$. The relation depends on the value of $\log g$, so for Trumpler 10 ($\log g \approx 4.3$) we use Eq. 2, and for Praesepe ($\log g \approx 4.0$) we use Eq. 3:

$$\tilde{T}^{\rm eff} = (3.5 \pm 0.1)\nu_{max}^{(\mu Hz)} + (6460 \pm 40)^{(K)} \quad (2)$$

$$\tilde{T}^{\rm eff} = (3.8 \pm 0.2)\nu_{max}^{(\mu Hz)} + (6750 \pm 40)^{(K)} \quad (3)$$

The estimated values for $\Delta\nu_{low}$, $\nu_{\rm max}$ and their corresponding seismic temperatures, $\tilde{T}^{\rm eff}$, for our sample of δ Sct stars in Trumpler 10 and Praesepe are shown in Table 4.

5. The grids of models

As δ Sct are usually moderate to fast rotators ($v \sin i > 100$ km s^{-1}), the models have to take into account the stellar structure

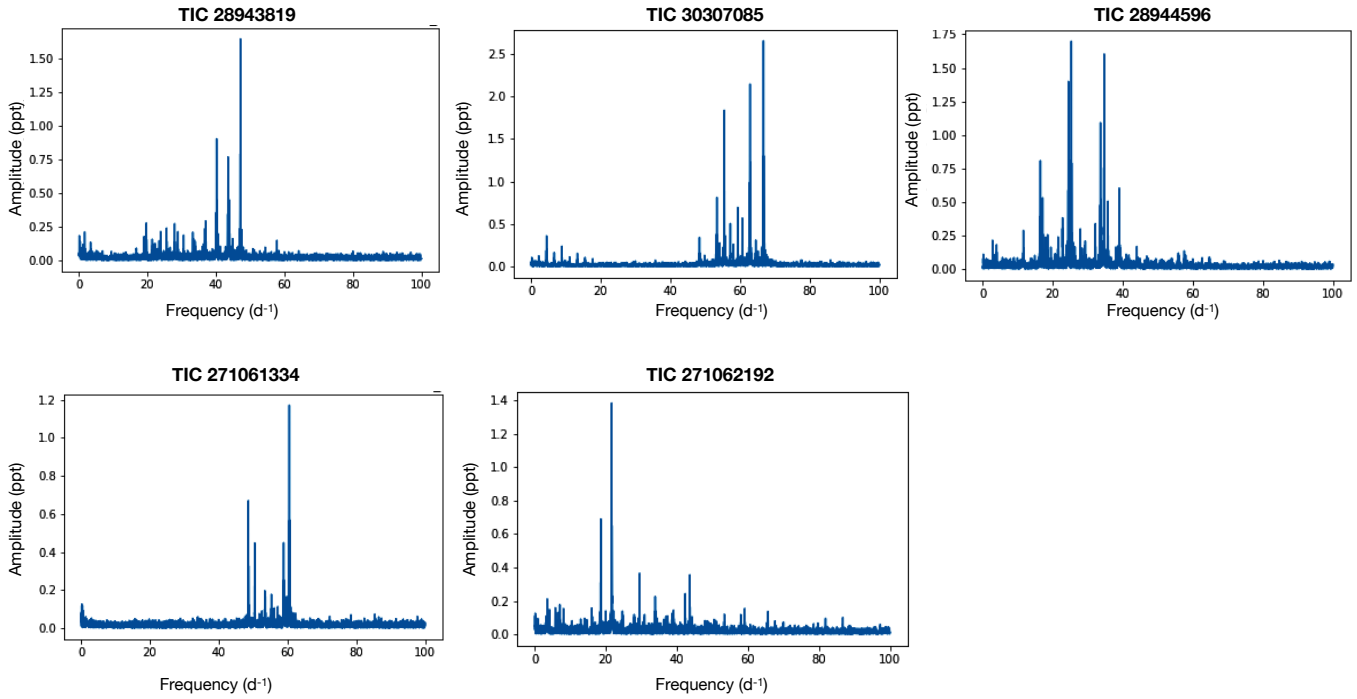

Fig. 1: Frequency spectrum of the sample of δ Sct stars candidates in the field of Trumpler 10

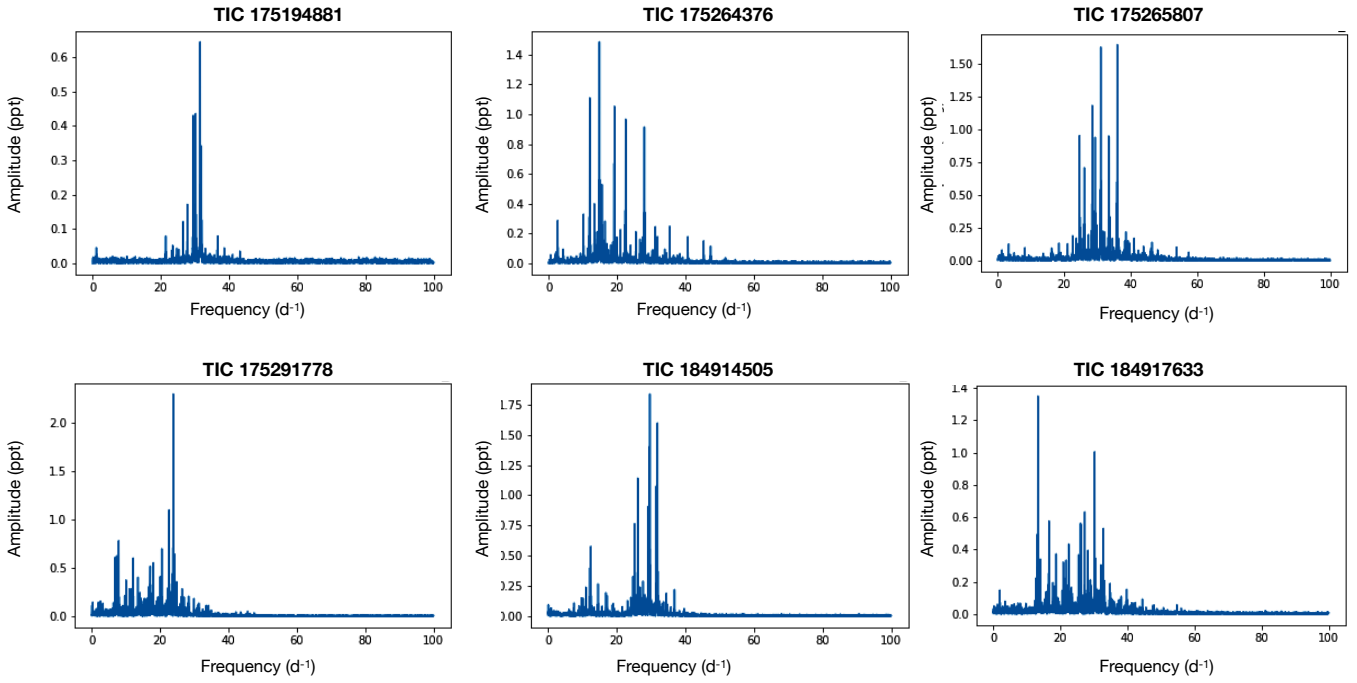

Fig. 2: Same as Fig. 1 for the Praesepe sample

deformation that occurs at these speeds. This centrifugal flattening reduces the value of the mean density, directly related to one of the seismic indices that we are using here, the large separation. For this reason, we calculate our models with the MESA code (Paxton 2019), and the related oscillations with the FILOU code (Suárez & Goupil 2008), taking rotation into account up to second order in the pertubative theory for the adiabatic oscillation computation (including near-degeneracy effects and stellar structure deformation).

Following DPO22, we build two grids of representative models to characterize δ Sct stars during their stay on MS, one for Trumpler 10 and another for Praesepe. In Table 5 we introduce their main parameters. The values for the initial angular velocity to critical velocity ratio are between $0.1\Omega_c$ and $0.5\Omega_c$, avoiding higher values that may lie beyond the limits of the perturbative theory. We compute p and g modes in the low-order regime, between $n = 1$ and $n = 8$, and with degrees between $l = 0$ and $l = 3$.

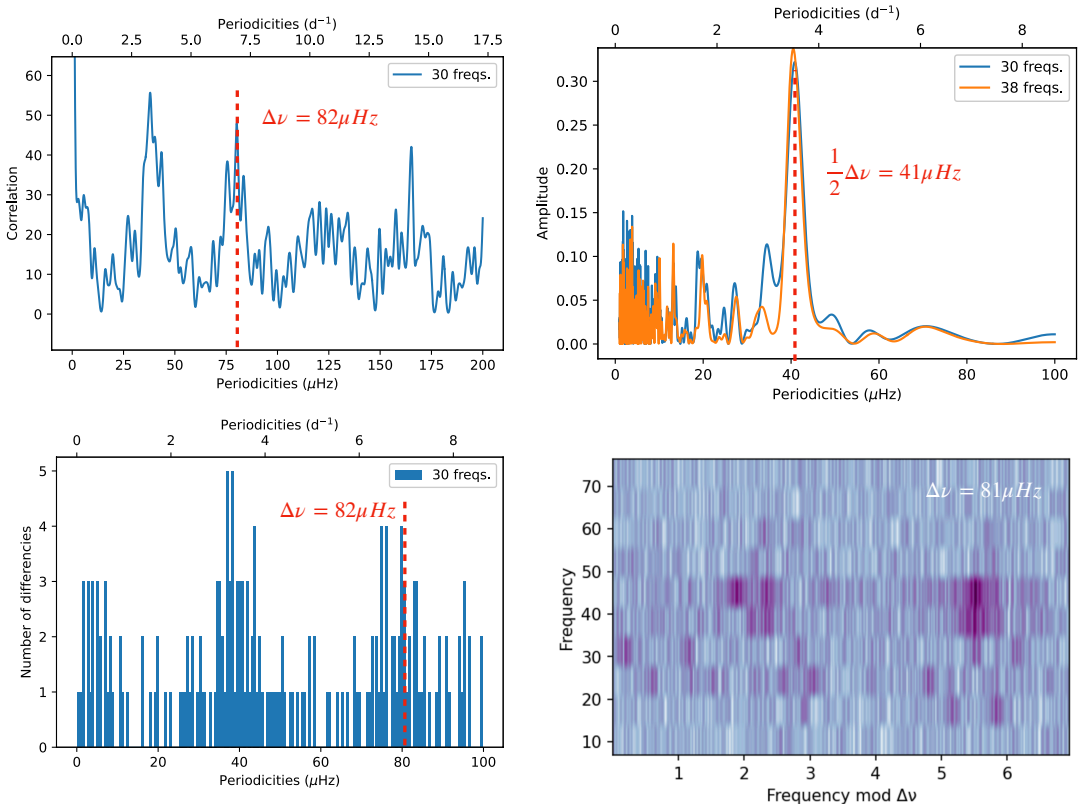

Fig. 3: Estimated low-order large separation for TIC 28943819, using the Autocorrelation Diagram (top left), the Discreet Fourier Transform (top right), the Frequency Difference Histogram (bottom left), and the échelle Diagram (Hey & Ball 2020) (bottom right)

Table 4: Seismic indices of the selected targets from Trumpler 10 and Praesepe: the low-order large separation, the frequency at maximum power and its corresponding seismic effective temperature

TIC	$\Delta\nu_{\rm low}(\mu$Hz)	$\nu_{\rm max}(\mu$Hz)	$\tilde{T}^{\rm eff}$ (K)
Trumpler 10			
28943819	82 ± 2	510 ± 30	8250 ± 200
30307085	84 ± 1	710 ± 60	8950 ± 320
28944596	80 ± 2	330 ± 80	7620 ± 350
271061334	80 ± 2	650 ± 50	8740 ± 280
271062192	76 ± 2	290 ± 90	7480 ± 380
Praesepe			
175194881	58 ± 1	350 ± 30	8080 ± 220
175264376	52 ± 3	210 ± 60	7550 ± 310
175265807	57 ± 2	360 ± 40	8120 ± 260
175291778	52 ± 3	200 ± 70	7510 ± 350
184914505	56 ± 1	320 ± 60	7970 ± 330
184917633	56 ± 1	270 ± 80	7780 ± 400

6. The method for estimating ages

We estimate the seismic age of each cluster following the next work flow:

1. For each star, we constrain the models using the estimated values of $\Delta\nu_{\rm low}$ and $\tilde{T}_{\rm eff}$ of the star.
2. We compute the ratios of the observed frequencies, in order to select the frequencies with ratios that match those of the models (Table 6).

Table 5: Parameters of the stellar model grids built with the MESA code. From top to bottom: mass, metallicity (both for Trumpler 10 and Praesepe), the initial angular velocity to critical velocity ratio and the mixing-length parameter

Parameter	Range	Step
M ($M_\odot$)	[1.60, 2.50]	0.01 $M_\odot$
Z (Trumpler 10)	[0.016, 0.020]	0.002
Z (Praesepe)	[0.028, 0.032]	0.002
Ω/Ω_c	[0.1, 0.5]	0.1
α	2.0	Fixed

3. Once we find a range of radial modes matching the observed frequencies, mainly the fundamental mode, we add the frequency ratios to the other seismic parameters to better constrain the stellar age.
4. After applying steps 1-3 to all stars in the same group, we plot the age distribution histograms of all the seismically constrained models.
5. Finally, we compute the best Kernel Density Estimation (KDE) over the age distribution, using an automatic algorithm to determine the best bandwidth value within a proposed interval (Pedregosa et al. 2011). This is a free parameter to fit the KDE to the distribution. A value too low leads to overfitting and the resulting function will be influenced by the noise in the data. On the contrary, a value too high will not reveal the underlying distribution function properly. We estimate the mean age, corresponding to the central peak of the distribution, and its corresponding standard deviation.

Table 6: The fundamental mode to radial overtone ratios in our MESA/FILOU grids of models, with their corresponding standard deviations

Relationship	Value with 1σ uncertainty
f_1/f_2	0.77 ± 0.01
f_1/f_3	0.63 ± 0.02
f_1/f_4	0.53 ± 0.02
f_1/f_5	0.45 ± 0.02
f_1/f_6	0.40 ± 0.02
f_1/f_7	0.35 ± 0.01
f_1/f_8	0.31 ± 0.01

Fig. 4 show the positions and the ranges of the possible radial overtones in the frequency spectrum of TIC 28943819 (see Appendix C for the rest of our sample). These ranges are too wide in some cases because we have sampled the whole grid for identification. Then, the inclusion of the fundamental mode has a minimal impact on the constraints we derive on the models, but it helps confirm what we obtain from the other seismic parameters. The method has failed, estimating the ranges for the possible radial overtones, only in the cases with fewer than 30 extracted significant frequencies: TIC 175194881 in Praesepe, and TIC 30307085 and TIC 271061334 in Trumpler 10.

7. Results and discussion

7.1. Trumpler 10

The HRD of Fig. 5 (left panel) shows the ages of the seismically constrained models of our sample of δ Sct stars in Trumpler 10. We can see that they are very close to the Zero Age Mean Sequence (ZAMS). Zooming in the area between 1.60 and 2.00 (Fig. 5, right panel), the models show that TIC 28944596 and TIC 271062192, the least massive stars of the sample, are older than the rest of the sample, in agreement with the observed larger radii and lower densities (Table 2). In the absence of data on the projected rotation velocity, it is unclear whether these stars are rapidly rotating or not.

To determine the mean age of the group, we investigate the age distribution histograms corresponding to every star of the sample, from the seismically constrained models (shown in Fig. 6, top left panel). We start by estimating a normal distribution over the ages of all the seismic constrained models, resulting in a mean age of 54 Myr (σ = 116%). This first approximation has allowed us to remove models older than 200 Myr, because they lie at a distance greater than 3σ from the central peak (Fig. 6, bottom left panel). We then estimate the mean age of the group by calculating the best possible distribution on the histograms, using a KDE with two different values of the bandwidth parameter (Fig. 6).

We see that the central peak coincides in both cases with 19 Myr (σ = 120%). A closer look at these histograms reveals that TIC 28944596 and TIC 271062192 deviate from the bell-shaped distribution followed by the other three stars. Removing these two discrepant stars from the sample reduces the uncertainty in the group age estimate by 28% without changing the mean age significantly, at 18 Myr (σ = 105%) when we consider only models with ages less than 200 Myr, as we can see in Fig. 6 (bottom left and bottom right panels). This is a younger age estimate than those referenced in Sect. 2. Uncertainties probably emerge because seismic parameters, including the large separation, evolve rapidly for stars on the pre-main sequence (PMS).

Recent theoretical works show that the PMS is a much more complex phase than previously thought. For example, Kunitomo et al. (2017) claim that the spread in luminosity can be explained through different efficiencies at which the accreted material is converted into internal energy for each star. This can explain the large uncertainty with which we estimate the age of this very young cluster. For these very young clusters, it seems that we need other parameters, in addition to the seismic ones we use, to date the stars with greater accuracy. This is confirmed by Steindl et al. (2022), according to which the evolution of the star along the PMS leaves an imprint on the frequency content of a δ Sct star. They claim that different PMS accretion scenarios cause differences in the pulsation modes. Seismology of PMS stars has a lot to say about their interior structure.

7.2. Praesepe

Fig. 7 (left panel) shows the HRD of the seismically constrained models for the δ Sct stars group in Praesepe. Two stars, TIC 175264376 and TIC 175291778, clearly appear to be older than the rest of the sample (right panel). This is more evident in Fig. 8, where we plot the age distribution histograms for every star of the sample. We estimate the best KDE using two different values for the bandwidth parameter. When the bandwith parameter is lower, a bimodality appears on the age distribution: TIC 175264376 and TIC 175291778 have a mean age of 870 ± 210 Myr, while the other four stars have a mean age of 585 ± 210 Myr.

The discrepant large separations and densities of TIC 175264376 and TIC 175291778 can be explained through rotation or a different age. On the one hand, a rapid rotation may modify the value of the large separation, although not the scaling relation between the large separation and the mean density (García Hernández et al. 2015; Mirouh et al. 2019). Their higher TIC radii and lower TIC densities (Table 3), are in line with the lower low-order large separations and frequencies at maximum power we estimate for both stars (Table 4), compared to the rest of the sample. The high value of the projected rotation velocity of TIC 175264376 (200 km s^{-1}) is very significant in this sense. Our 1D models cannot be applied to such high rotational velocities reliably. We then need 2D models to characterize rapidly-rotating stars. On the other hand, these bigger and lower-density stars with masses similar to the others, can also simply be more evolved. In Table 3 we can see that these stars, plus TIC 175194881, may be late A or earlier F stars, while the other four may be middle A stars, according to Fossati et al. (2008). They also show different surface metallicities. These could point to two different populations of stars. If we assume that all of them have a similar metallicity and age, then a unique population emerges, with mean age 780 ± 290 Myr, in good agreement with the majority of the references cited in Sect. 2. But deriving this estimate requires a larger bandwidth in the KDE, thus yielding a larger uncertainty than with Trumpler 10. In a more evolved cluster as Praesepe, rotation and other internal mixing phenomena can affect the stars differently over time.

As we can see in Table 7 and Table 8, the models are not well constrained in terms of rotational velocity. Estimating the rotation rate of some stars of the group would yield further constraints on the models, especially given the dependence of the seismic parameters such as the large separation or the frequency ratios on rotation (Suárez et al. 2006). Then, to advance this strategy, we need a method to help us confidently interpret the rotation frequency in the dense frequency spectrum of δ Sct stars. Also it is crucial to obtain a more reliable mode identification,

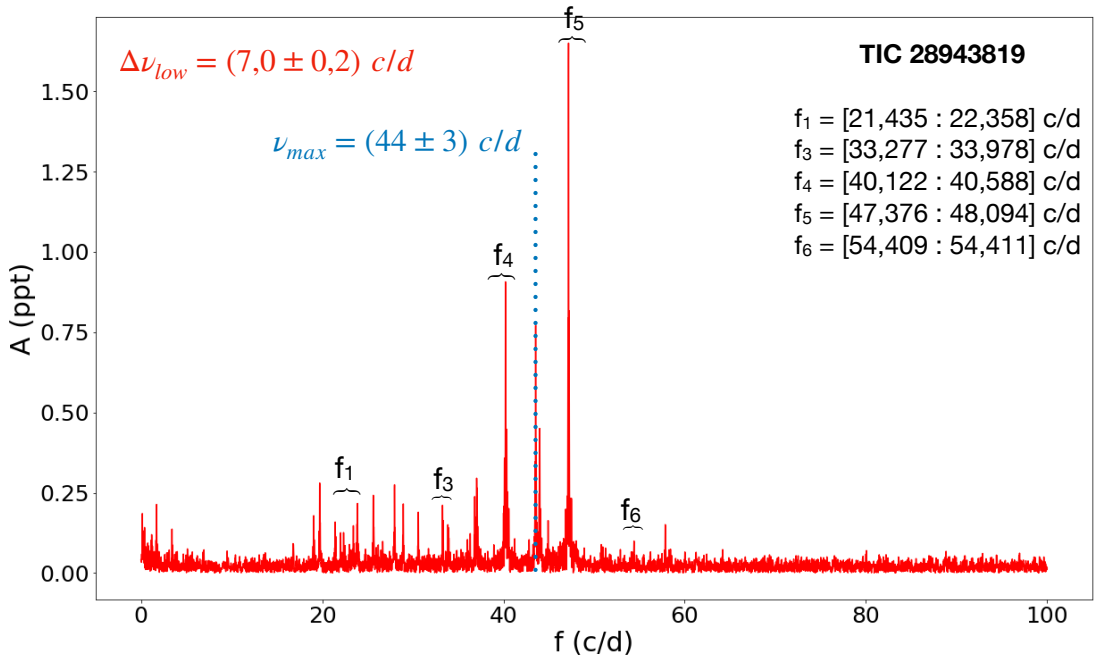

Fig. 4: Ranges for the possible radial overtones in the frequency spectrum of TIC 28943819

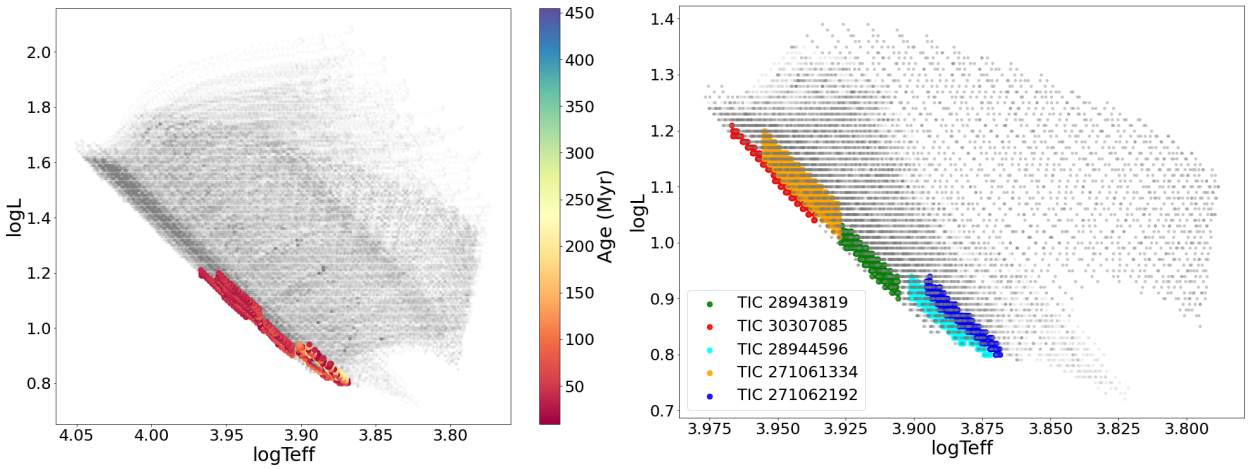

Fig. 5: Left: HRDs of the evolutionary tracks of our grid of representative models for the sample of δ Sct stars in Trumpler 10, the ages of the seismically constrained models have been color coded. Right: Zoom between 1.60 $M(M_\odot)$ and 2.00 $M(M_\odot)$, distinguishing between models for each of the stars in the sample by different colours

through high cadence observations that allow a higher resolution in the frequency spectrum. We hope that future missions, such as the ESA projects PLATO[4] ("PLAnetary Transits and Oscillations of stars") (Rauer et al. 2014) and HAYDN ("High-precision AsteroseismologY in DeNse stellar fields")[5] (Miglio et al. 2021), will provide high-cadence photometry of stars belonging to clusters, leading to accurate age estimates.

8. Conclusions

The use of asteroseismology to date young open clusters provides promising results, despite the limitations of statistical techniques applied to samples with such small numbers of stars. We have tested a seismic method with three open clusters of different ages. With α Per we obtained the first results in Pamos Ortega et al. (2022). In this work we extend the research to Trumpler 10 and Praesepe, and we have applied a method for identifying radial overtones.

Regarding Trumpler 10, we find five δ Sct stars candidates never before classified as such, with a mean age of 19 ± 22 Myr. The uncertainty is large due to how close they are to the PMS. If we stay only with the PMS models, uncertainty would be reduced by up to 40 %, but we need more evidences to ensure that they really are PMS stars.

Regarding Praesepe, we find a new possible δ Scuti star, TIC 184917633, that we add to our sample of five well known δ Sct stars. We estimate the mean age of this star group to 780 ± 290 Myr, in good agreement with the literature. Two of the six stars in the sample seem to be older than the rest. The dif-

[4] https://sci.esa.int/web/plato
[5] http://www.asterochronometry.eu/haydn/

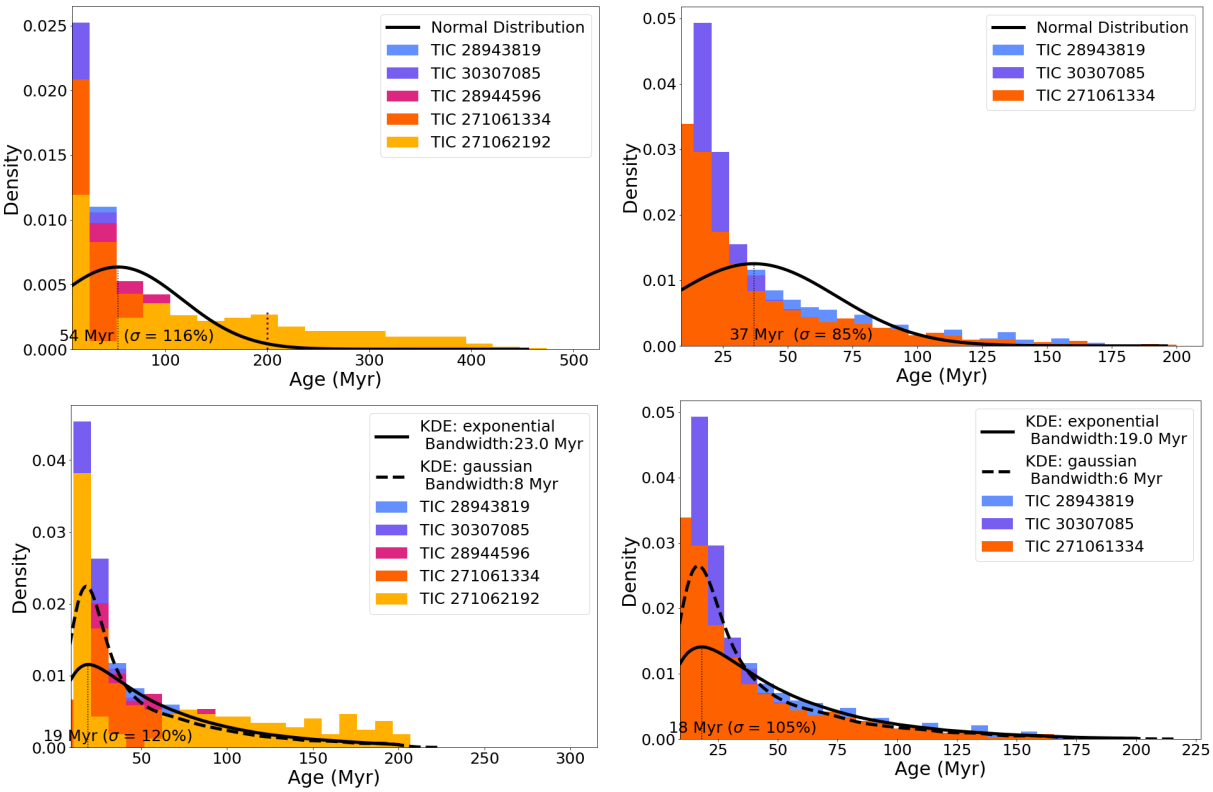

Fig. 6: Age distribution histograms of our sample of stars in Trumpler 10. Top left: The black solid line shows the normal distribution as a first approximation to the mean age (54 Myr, σ = 116%). Bottom left: Seismically constrained models younger than 200 Myr. The black solid line shows the KDE with a bandwidth of 23 Myr, and the black dashed line shows the KDE with a bandwidth of 8 Myr. The mean age of the group is 19 Myr (σ = 120%). Top right: Seismically constrained models for TIC 28943819, TIC 30307085 and TIC 271061334. The black solid line shows the normal distribution as a first approximation to the mean age (37 Myr, σ = 85%). Bottom right: Seismically constrained models younger than 200 Myr, for TIC 28943819, TIC 30307085 and TIC 271061334. The black solid line shows the KDE with a bandwidth of 19 Myr, and the black dashed line the KDE with a bandwidth of 6 Myr. The mean age of the group is 18 Myr (σ = 105%)

Table 7: Constrained parameters of the models corresponding to our selected targets in Trumpler 10, with their corresponding standard deviations

TIC	$M(M_\odot)$	$R(R_\odot)$	$\bar{\rho}(\bar{\rho}_\odot)$	log g	$\tilde{T}^{\rm eff}(K)$	$log(L/L_\odot)$	v_{rot}(km s^{-1})	Age (Myr)
28943819	1.72 ± 0.03	1.51 ± 0.02	0.50 ± 0.01	4.32 ± 0.01	8250 ± 110	0.97 ± 0.03	80 ± 40	40 ± 40
30307085	1.86 ± 0.04	1.53 ± 0.02	0.52 ± 0.01	4.34 ± 0.01	8920 ± 180	1.12 ± 0.04	60 ± 20	25 ± 15
28944596	1.64 ± 0.03	1.52 ± 0.02	0.47 ± 0.01	4.29 ± 0.01	7770 ± 130	0.87 ± 0.03	80 ± 40	60 ± 50
271061334	1.86 ± 0.04	1.58 ± 0.03	0.47 ± 0.02	4.31 ± 0.01	8730 ± 160	1.11 ± 0.04	80 ± 50	40 ± 30
271062192	1.64 ± 0.03	1.56 ± 0.01	0.43 ± 0.01	4.27 ± 0.01	7670 ± 120	0.88 ± 0.03	110 ± 50	70 ± 60

ferent values in their parameters, especially the metallicity and the spectral type, support the thesis of two stellar populations: one with a mean age of 590 ± 210 Myr and another with a mean age of 870 ± 210 Myr. This apparent bimodality in the age distribution could also be due to these stars' rapid rotation. The lower values in the low-order large separation and the frequency at maximum power, in addition to the measured large projected rotation velocity of both stars, support this idea. The 1D models that we have used in this work are not the most suitable to stars with such a high rotation. Two-dimensional models are needed in order to take more into account the deformation that occurs in them, and that greatly impact the seismic parameters, such as the large separation and a reliable determination of the rotation frequency.

Acknowledgements. DPO and AGH acknowledge funding support from 'FEDER/junta de Andalucía-Consejería de Economía y Conocimiento' under project E-FQM-041-UGR18 by Universidad de Granada. JCS, GMM and SBF acknowledge funding support from the Spanish State Research Agency (AEI) project PID2019-107061GB-064. This paper includes data collected with the TESS mission, obtained from the TASC data archive. Funding for the TESS mission is provided by the NASA Explorer Program. STScI is operated by the Association of Universities for Research in Astronomy, Inc., under NASA contract NAS 5–26555.

References

Barceló Forteza, S., Moya, A., Barrado, D., et al. 2020, A&A, 638, A59
Barceló Forteza, S., Roca Cortés, T., & García, R. A. 2018, A&A, 614, A46
Barnes, S. A. 2003, ApJ, 586, 464

Table 8: Same as Table 7 for the Praesepe sample

TIC	$M(M_\odot)$	$R(R_\odot)$	$\bar{\rho}(\bar{\rho}_\odot)$	$\log g$	$\tilde{T}^{\rm eff}(K)$	$log(L/L_\odot)$	v_{rot}(km s^{-1})	Age (Myr)
175194881	1.83 ± 0.03	1.92 ± 0.03	0.26 ± 0.01	4.13 ± 0.01	7680 ± 100	1.06 ± 0.03	120 ± 60	500 ± 110
175264376	1.73 ± 0.05	2.03 ± 0.06	0.21 ± 0.01	4.06 ± 0.02	7200 ± 160	0.99 ± 0.05	110 ± 50	880 ± 120
175265807	1.85 ± 0.04	1.94 ± 0.03	0.25 ± 0.01	4.13 ± 0.01	7720 ± 130	1.08 ± 0.04	120 ± 60	510 ± 110
175291778	1.72 ± 0.05	2.02 ± 0.06	0.21 ± 0.02	4.06 ± 0.02	7160 ± 180	0.98 ± 0.06	110 ± 50	900 ± 140
184914505	1.81 ± 0.05	1.96 ± 0.03	0.24 ± 0.01	4.11 ± 0.01	7580 ± 160	1.05 ± 0.05	120 ± 50	600 ± 100
184917633	1.76 ± 0.06	1.93 ± 0.03	0.24 ± 0.01	4.11 ± 0.01	7410 ± 200	1.00 ± 0.06	130 ± 50	640 ± 120

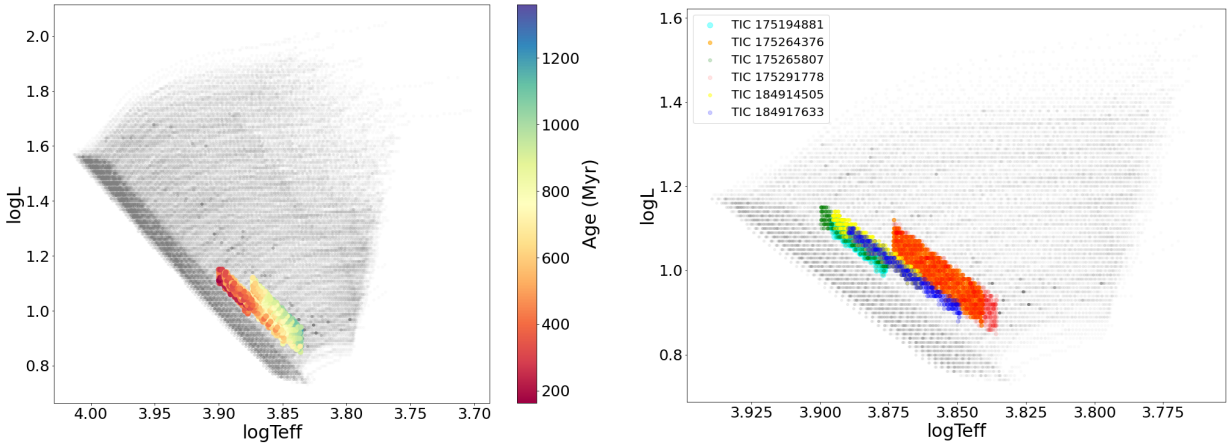

Fig. 7: The same as Fig. 5 for Praesepe

Basri, G. & Martín, E. L. 1999, ApJ, 510, 266
Bastian, N. & Lardo, C. 2018, ARA&A, 56, 83
Bedding, T. R., Murphy, S. J., Hey, D. R., et al. 2020, Nature, 581, 147
Bochanski, J. J., Faherty, J. K., Gagné, J., et al. 2018, AJ, 155, 149
Bowman, D. M. & Kurtz, D. W. 2018, MNRAS, 476, 3169
Brandt, T. D. & Huang, C. X. 2015, ApJ, 807, 24
Breger, M., Stich, J., Garrido, R., et al. 1993, A&A, 271, 482
Cantat-Gaudin, T., Jordi, C., Vallenari, A., et al. 2018, A&A, 618, A93
Choi, J., Dotter, A., Conroy, C., et al. 2016, ApJ, 823, 102
Costa, G., Girardi, L., Bressan, A., et al. 2019, A&A, 631, A128
Cummings, J. D., Deliyannis, C. P., Maderak, R. M., & Steinhauer, A. 2017, AJ, 153, 128
Cummings, J. D., Kalirai, J. S., Tremblay, P. E., Ramirez-Ruiz, E., & Choi, J. 2018, ApJ, 866, 21
da Silva, R., Porto de Mello, G. F., Milone, A. C., et al. 2012, A&A, 542, A84
Dias, W. S., Monteiro, H., Moitinho, A., et al. 2021, MNRAS, 504, 356
Douglas, S. T., Curtis, J. L., Agüeros, M. A., et al. 2019, ApJ, 879, 100
Fossati, L., Bagnulo, S., Landstreet, J., et al. 2008, A&A, 483, 891
Gaia Collaboration, Babusiaux, C., van Leeuwen, F., et al. 2018, A&A, 616, A10
García Hernández, A., Martín-Ruiz, S., Monteiro, M. J. P. F. G., et al. 2015, ApJ, 811, L29
García Hernández, A., Moya, A., Michel, E., et al. 2009, A&A, 506, 79
García Hernández, A., Moya, A., Michel, E., et al. 2013, A&A, 559, A63
García Hernández, A., Suárez, J. C., Moya, A., et al. 2017, MNRAS, 471, L140
Grigahcène, A., Antoci, V., Balona, L., et al. 2010, ApJ, 713, L192
Hasanzadeh, A., Safari, H., & Ghasemi, H. 2021, MNRAS, 505, 1476
Hey, D. & Ball, W. 2020, Echelle: Dynamic echelle diagrams for asteroseismology
Kharchenko, N. V., Piskunov, A. E., Schilbach, E., Röser, S., & Scholz, R. D. 2013, A&A, 558, A53
Krause, M. G. H., Offner, S. S. R., Charbonnel, C., et al. 2020, Space Science Reviews, 216
Kunitomo, M., Guillot, T., Takeuchi, T., & Ida, S. 2017, A&A, 599, A49
Martín, E. L., Dahm, S., & Pavlenko, Y. 2001, in Astronomical Society of the Pacific Conference Series, Vol. 245, Astrophysical Ages and Times Scales, ed. T. von Hippel, C. Simpson, & N. Manset, 349
Meibom, S. & Mathieu, R. D. 2005, ApJ, 620, 970
Miglio, A., Girardi, L., Grundahl, F., et al. 2021, Experimental Astronomy, 51, 963
Mirouh, G. M., Angelou, G. C., Reese, D. R., & Costa, G. 2019, MNRAS, 483, L28
Moya, A., Sarro, L. M., Delgado-Mena, E., et al. 2022, A&A, 660, A15
Netopil, M., Paunzen, E., Heiter, U., & Soubiran, C. 2016, A&A, 585, A150
Pamos Ortega, D., García Hernández, A., Suárez, J. C., et al. 2022, MNRAS, 513, 374
Paparó, M., Benkő, J. M., Hareter, M., & Guzik, J. A. 2016, ApJ, 822, 100
Paxton, B. 2019, Modules for Experiments in Stellar Astrophysics (MESA)
Pedregosa, F., Varoquaux, G., Gramfort, A., et al. 2011, Journal of Machine Learning Research, 12, 2825
Press, W. H. & Rybicki, G. B. 1989, ApJ, 338, 277
Ramón-Ballesta, A., García Hernández, A., Suárez, J. C., et al. 2021, MNRAS, 505, 6217
Rauer, H., Catala, C., Aerts, C., et al. 2014, Experimental Astronomy, 38, 249
Reese, D. R., Lignières, F., Ballot, J., et al. 2017, A&A, 601, A130
Ricker, G. R., Winn, J. N., Vanderspek, R., et al. 2014, in Society of Photo-Optical Instrumentation Engineers (SPIE) Conference Series, Vol. 9143, Proc. SPIE, 914320
Skiff, B. A. 2014, VizieR Online Data Catalog, B/mk
Spina, L., Meléndez, J., Karakas, A. I., et al. 2017, Monthly Notices of the Royal Astronomical Society, 474, 2580
Stassun, K. G. 2019, VizieR Online Data Catalog, IV/38
Stauffer, J. R., Barrado y Navascués, D., Bouvier, J., et al. 1999, ApJ, 527, 219
Steindl, T., Zwintz, K., & Vorobyov, E. 2022, Nature Communications, 13, 5355
Suárez, J. C., García Hernández, A., Moya, A., et al. 2014, A&A, 563, A7
Suárez, J. C., Garrido, R., & Goupil, M. J. 2006, A&A, 447, 649
Suárez, J. C. & Goupil, M. J. 2008, Ap&SS, 316, 155
Suárez, J. C., Michel, E., Pérez Hernández, F., et al. 2002, A&A, 390, 523
Uytterhoeven, K., Moya, A., Grigahcène, A., et al. 2011, A&A, 534, A125
Zhong, J., Chen, L., Wu, D., et al. 2020, A&A, 640, A127

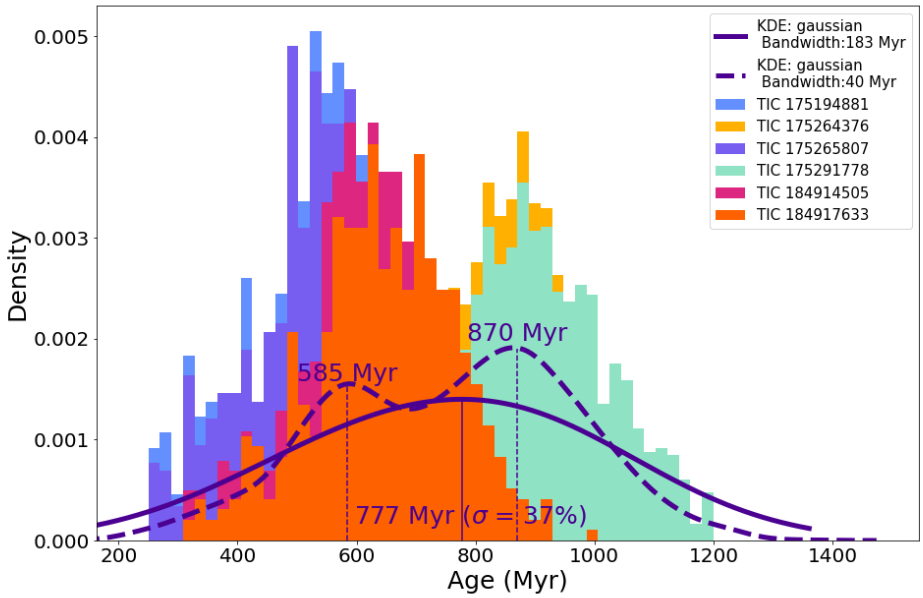

Fig. 8: Age distribution histograms for the seismically constrained models of our sample of stars in Praesepe 10. The black solid line is a KDE with a bandwidth parameter of 183 Myr. The mean age of the entire group is around 777 Myr (σ = 37%). The black dashed line shows a KDE bimodal distribution with a bandwidth of 40 Myr, revealing two age discrepant stars with respect to the other four: TIC 175264376 and TIC 175291778 have a mean age of around 870 Myr, and TIC 175194881, TIC 175265807, TIC 184914505 and TIC 184917633 seem to be younger, with a mean age of around 585 Myr

Appendix A The ten extracted highest amplitudes frequencies of our δ Sct stars sample

Table A.1: Ten extracted highest amplitudes frequencies, for each star in our samples of Trumpler 10 and Praesepe

Trumpler 10			Praesepe		
TIC	$f(d^{-1})$	A (ppt)	TIC	$f(d^{-1})$	A (ppt)
TIC 28943819	47.185	1.667	TIC 175194881	31.566	0.645
	40.230	0.885		30.242	0.314
	43.554	0.787		29.507	0.426
	44.008	0.463		31.896	0.351
	40.122	0.342		27.811	0.168
	40.359	0.335		26.556	0.117
	37.046	0.318		36.742	0.079
	19.721	0.282		21.457	0.081
	27.977	0.277		23.489	0.051
	36.830	0.251		38.623	0.047
TIC 30307085	66.752	2.630	TIC 175264376	14.845	1.471
	62.280	2.009		12.021	0.914
	55.489	1.809		19.260	1.055
	53.359	0.810		22.514	0.971
	59.387	0.703		27.996	0.919
	60.692	0.548		19.167	0.610
	57.244	0.448		15.575	0.511
	4.427	0.359		13.359	0.394
	48.369	0.344		10.180	0.339
	64.533	0.292		16.501	0.292
TIC 28944596	25.341	1.674	TIC 175265807	35.980	1.629
	34.691	1.588		31.020	1.618
	24.494	1.358		28.457	1.200
	33.649	1.089		24.659	0.975
	16.494	0.815		29.333	0.949
	39.021	0.682		33.417	0.829
	17.145	0.535		33.544	0.812
	35.790	0.513		26.086	0.708
	22.821	0.398		33.794	0.300
	32.201	0.344		28.901	0.262
TIC 271061334	60.529	1.163	TIC 175291778	23.855	2.336
	48.627	0.684		22.667	1.093
	58.877	0.474		7.908	0.790
	50.485	0.455		20.512	0.702
	53.414	0.201		7.332	0.640
	55.330	0.192		24.209	0.631
	53.583	0.168		6.827	0.612
	59.792	0.147		12.141	0.609
	60.696	0.134		18.050	0.546
	0.212	0.157		17.146	0.519
TIC 271062192	21.680	1.397	TIC 184914505	29.667	1.849
	18.611	0.703		31.899	1.543
	29.522	0.367		29.465	1.138
	43.681	0.351		26.145	1.168
	42.380	0.238		31.565	1.059
	33.928	0.224		29.257	0.869
	3.527	0.209		25.231	0.782
	7.028	0.178		12.482	0.591
	59.146	0.157		12.233	0.417
	5.777	0.154		27.690	0.323
			TIC 184917633	13.309	1.359
				30.241	1.019
				27.305	0.613
				16.610	0.581
				26.031	0.531
				32.840	0.526
				26.241	0.518
				22.494	0.435
				13.192	0.402
				28.240	0.409

Appendix B The estimated large separations of our δ Sct stars sample

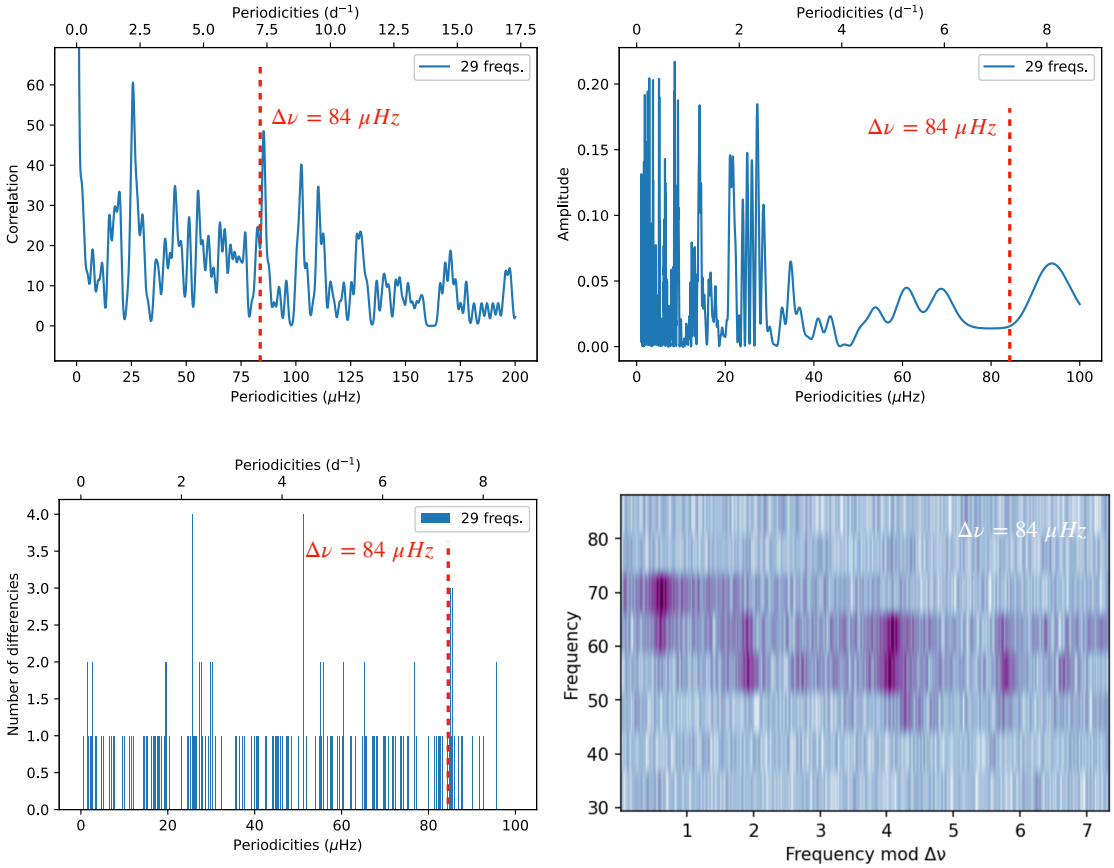

Fig. B.1: The same as Fig. 3 for TIC 30307085

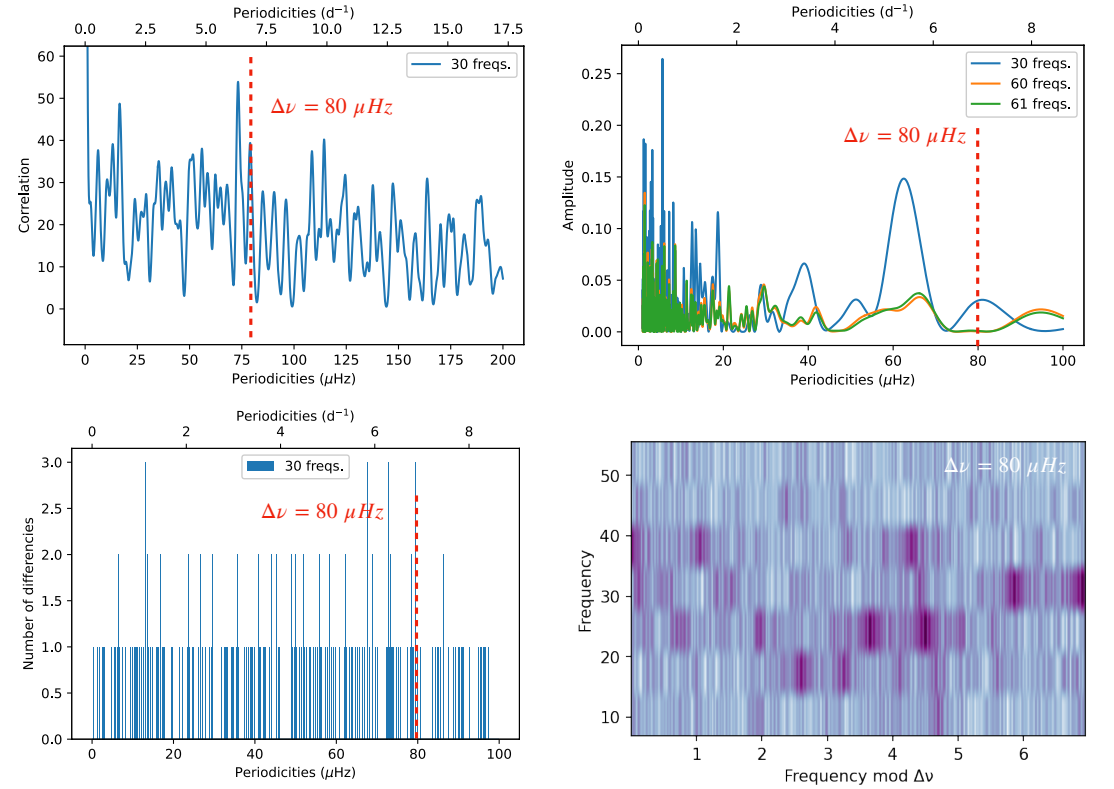

Fig. B.2: The same as Fig. 3 for TIC 28944596

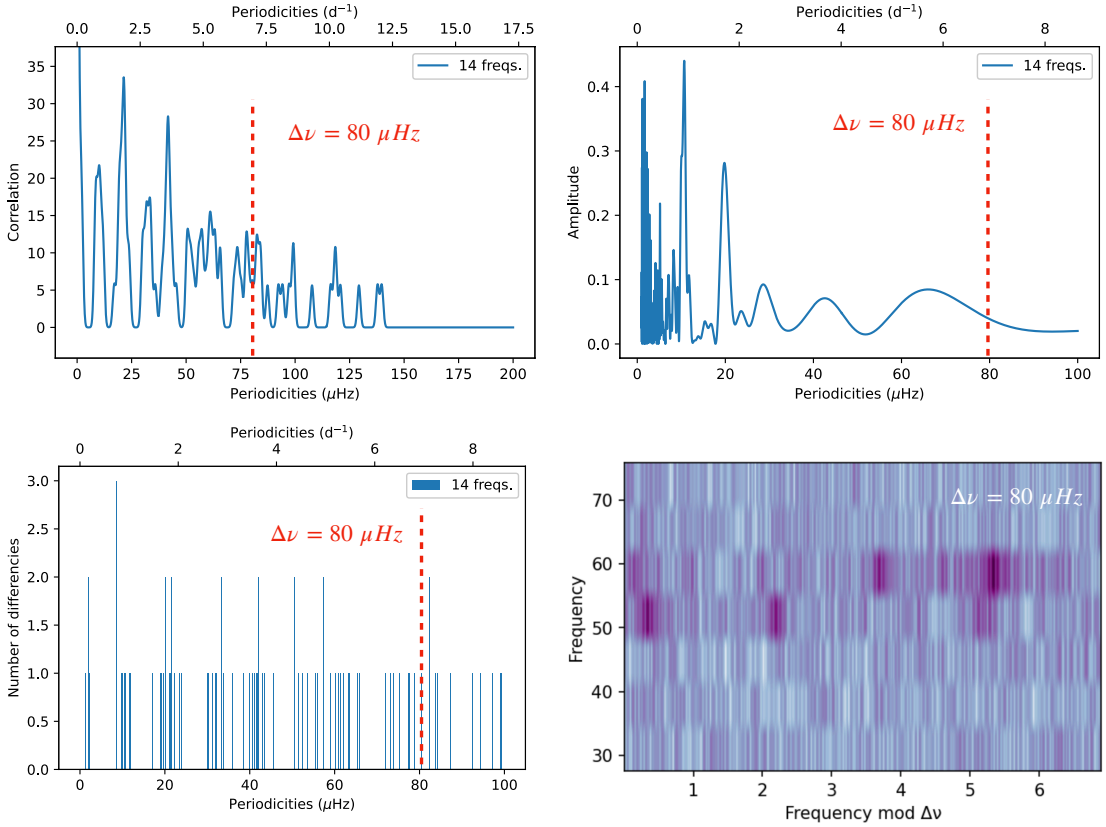

Fig. B.3: The same as Fig. 3 for TIC 271061334

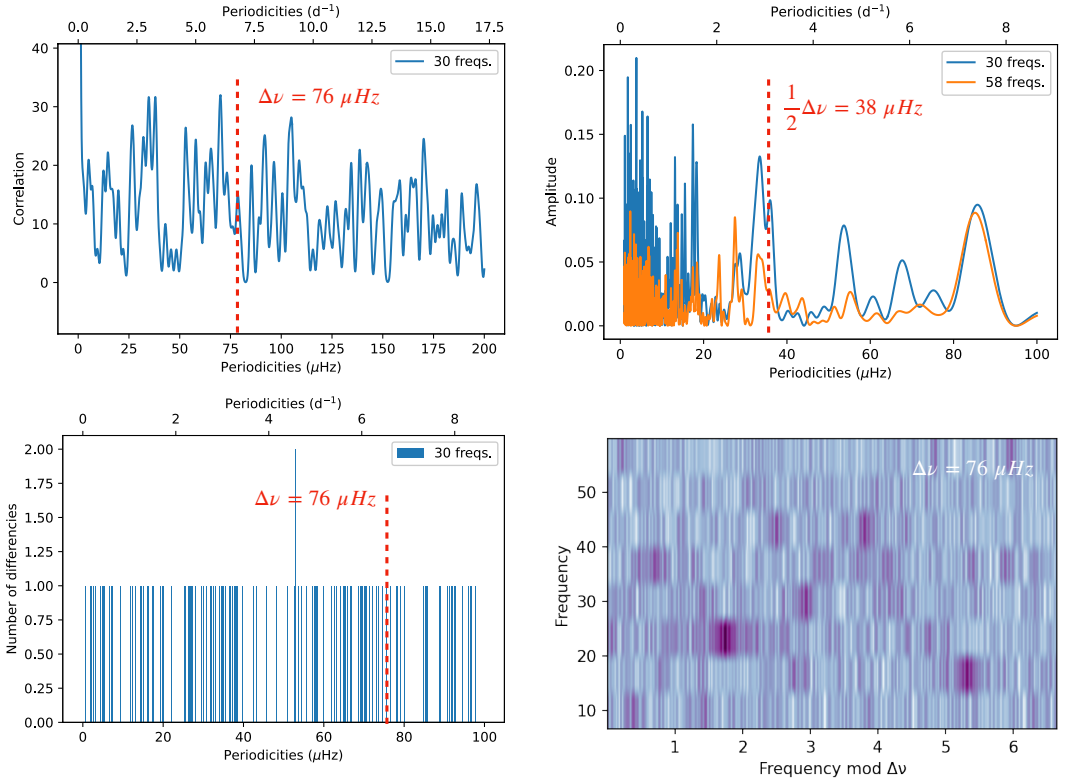

Fig. B.4: The same as Fig. 3 for TIC 271062192

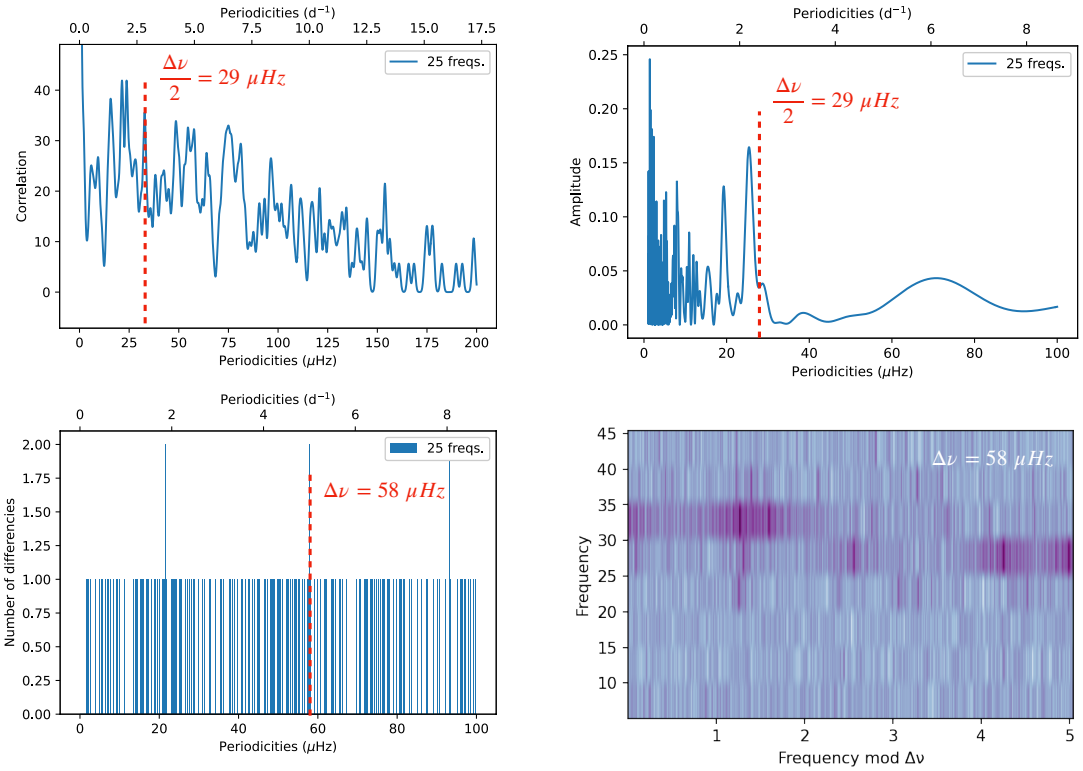

Fig. B.5: The same as Fig. 3 for TIC 175194881

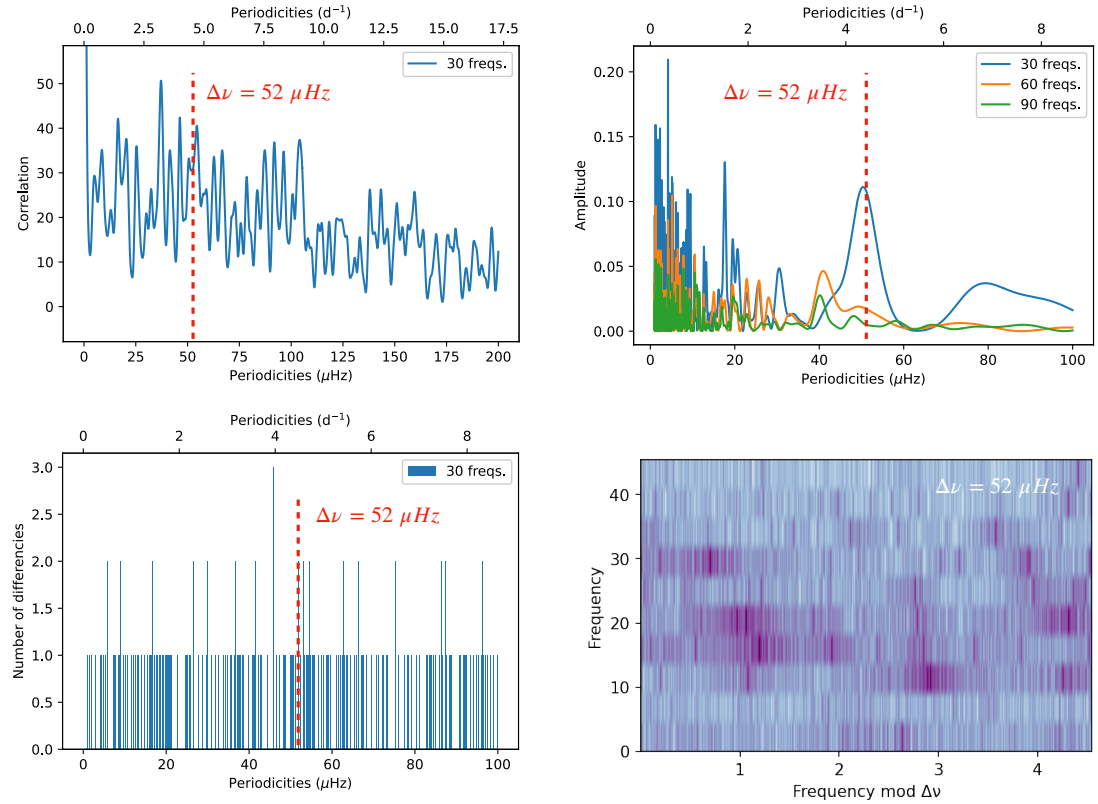

Fig. B.6: The same as Fig. 3 for TIC 175264376

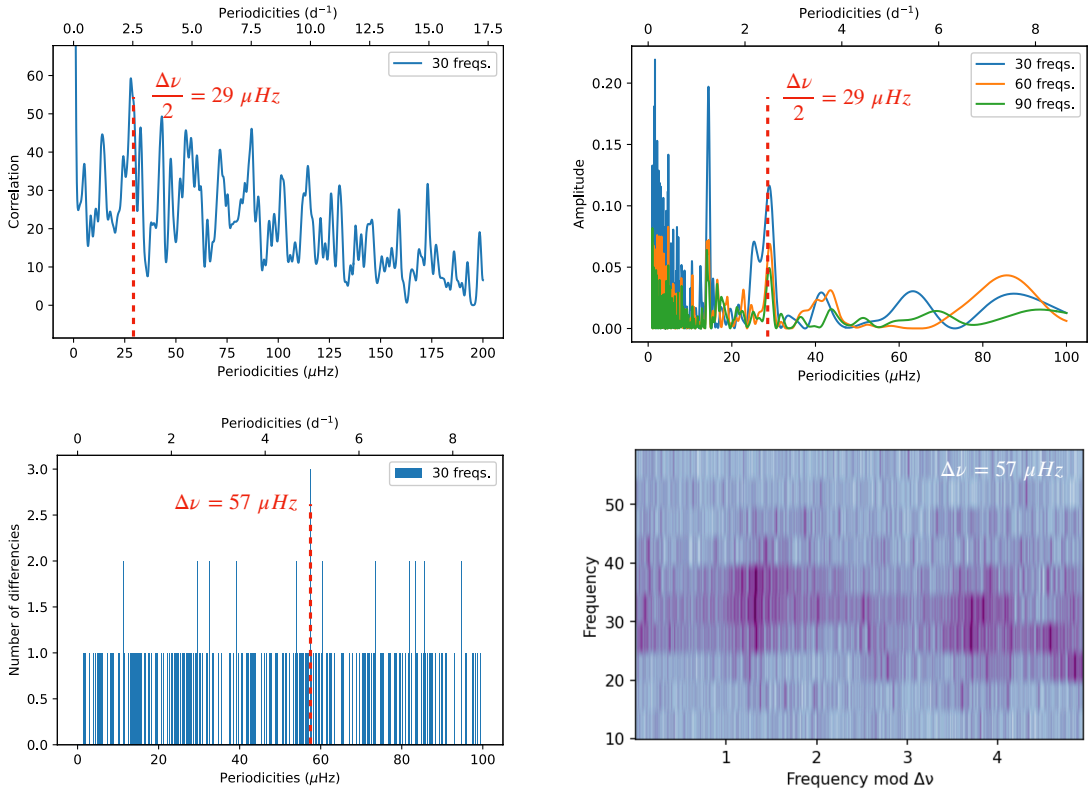

Fig. B.7: The same as Fig. 3 for TIC 175265807

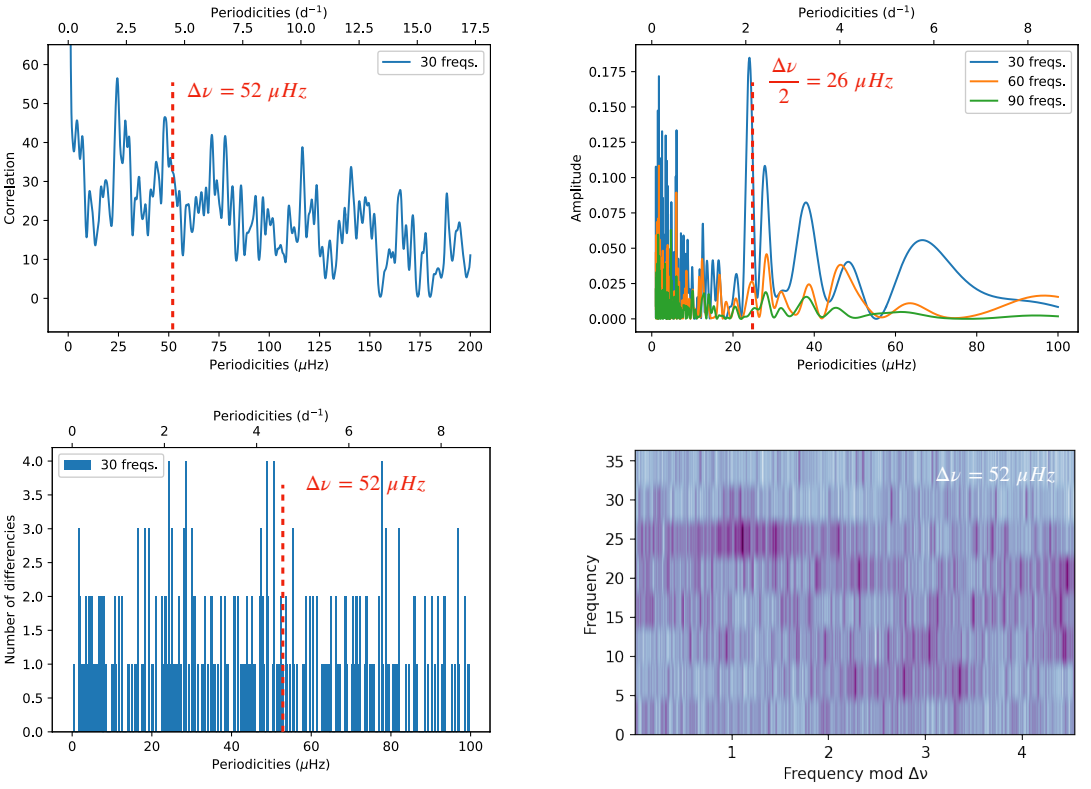

Fig. B.8: The same as Fig. 3 for TIC 175291778

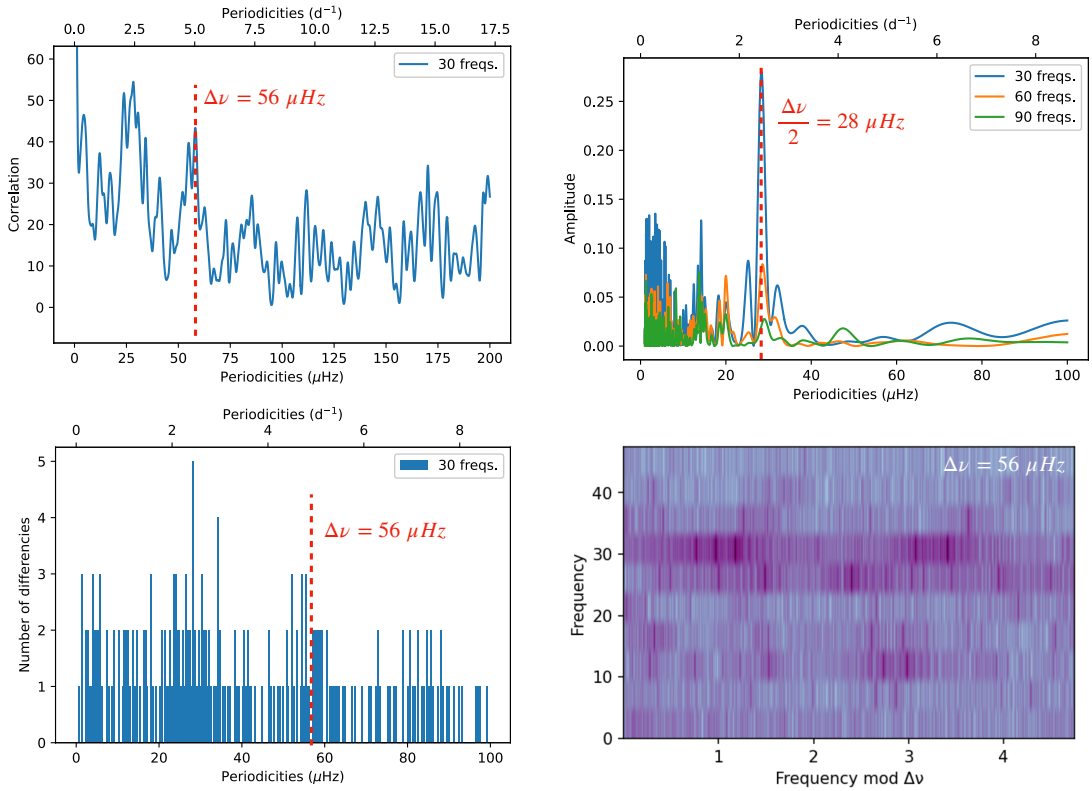

Fig. B.9: The same as Fig. 3 for TIC 184914505

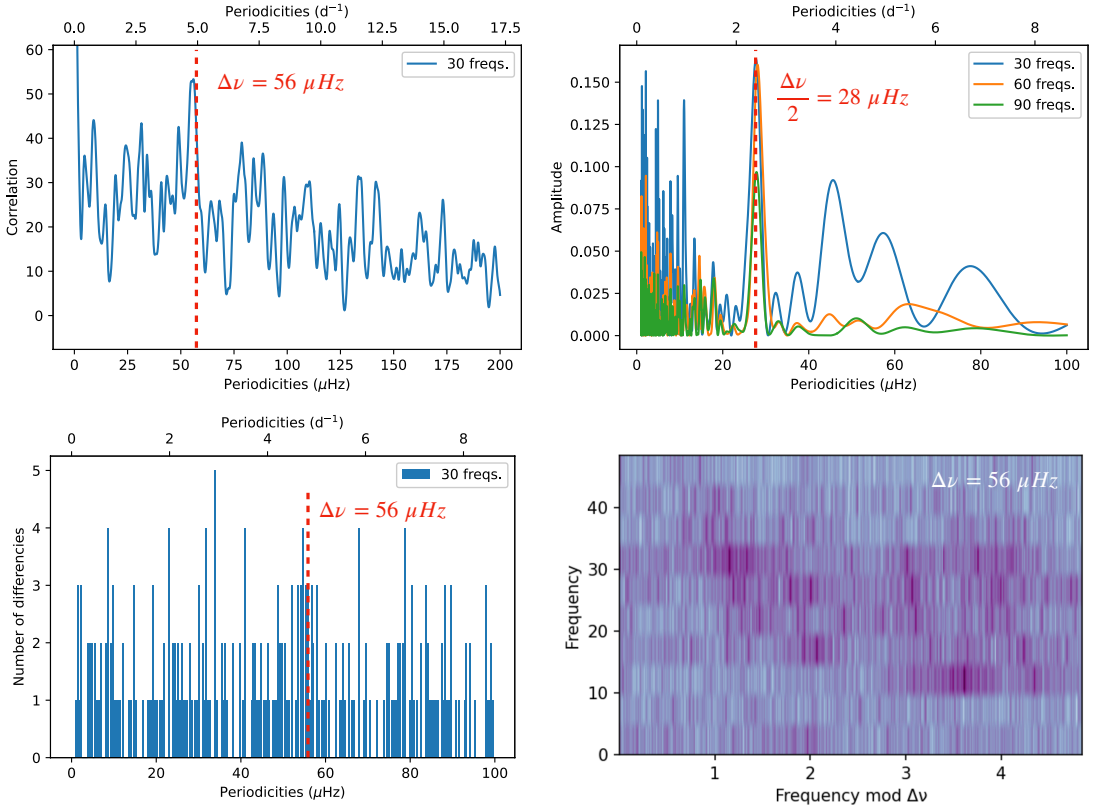

Fig. B.10: The same as Fig. 3 for TIC 184917633

Appendix C The positions and ranges of the possible radial modes of our δ Sct stars sample

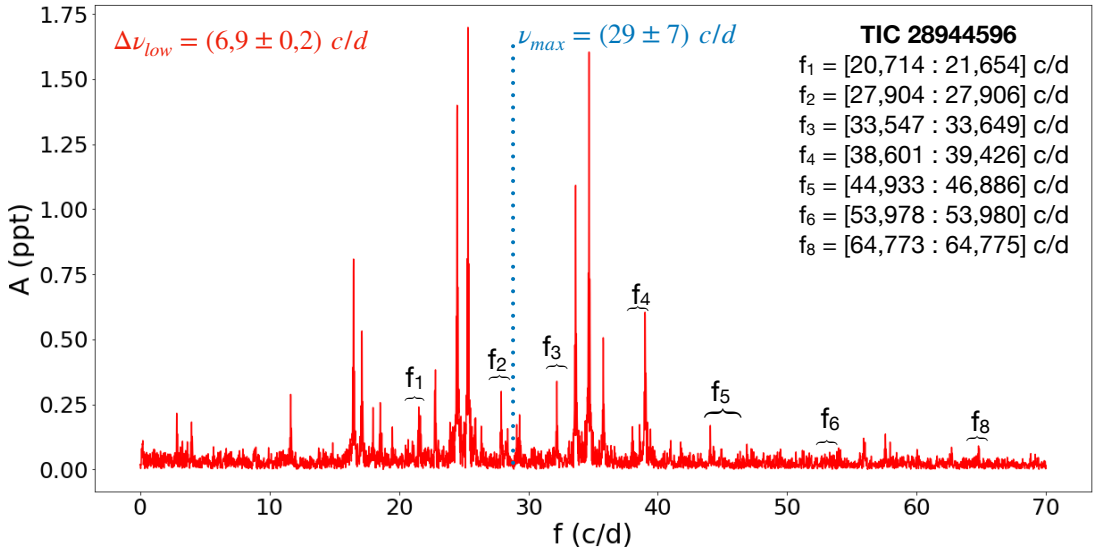

Fig. C.1: The same as Fig. 4 for TIC 28944596

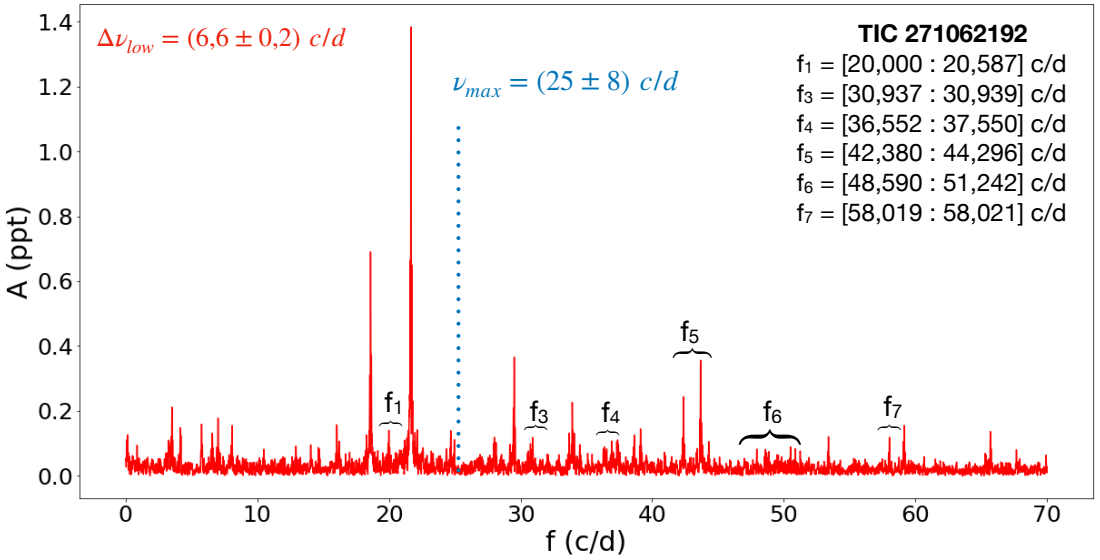

Fig. C.2: The same as Fig. 4 for TIC 271062192

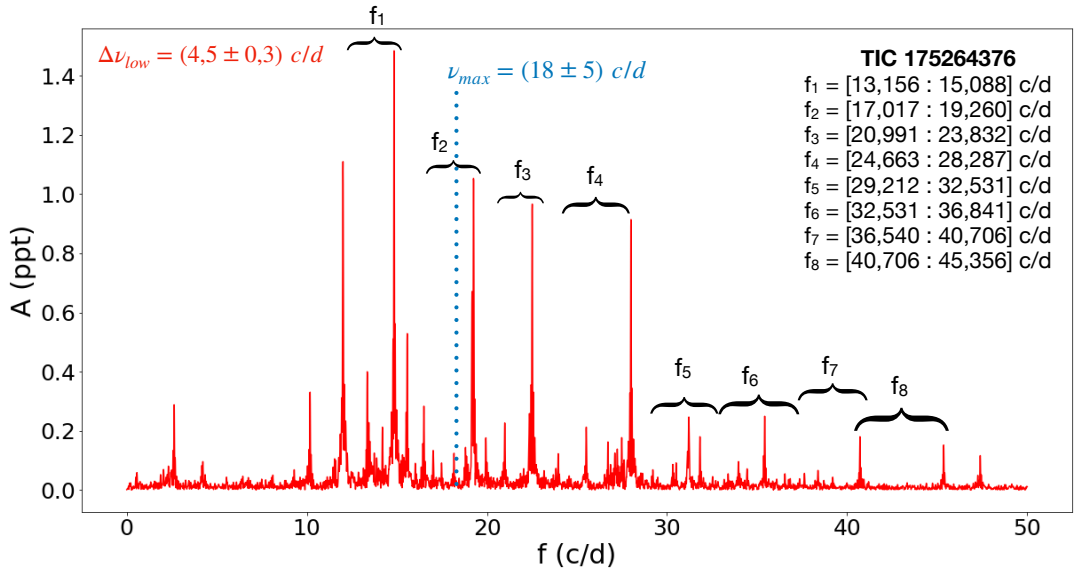

Fig. C.3: The same as Fig. 4 for TIC 175264376

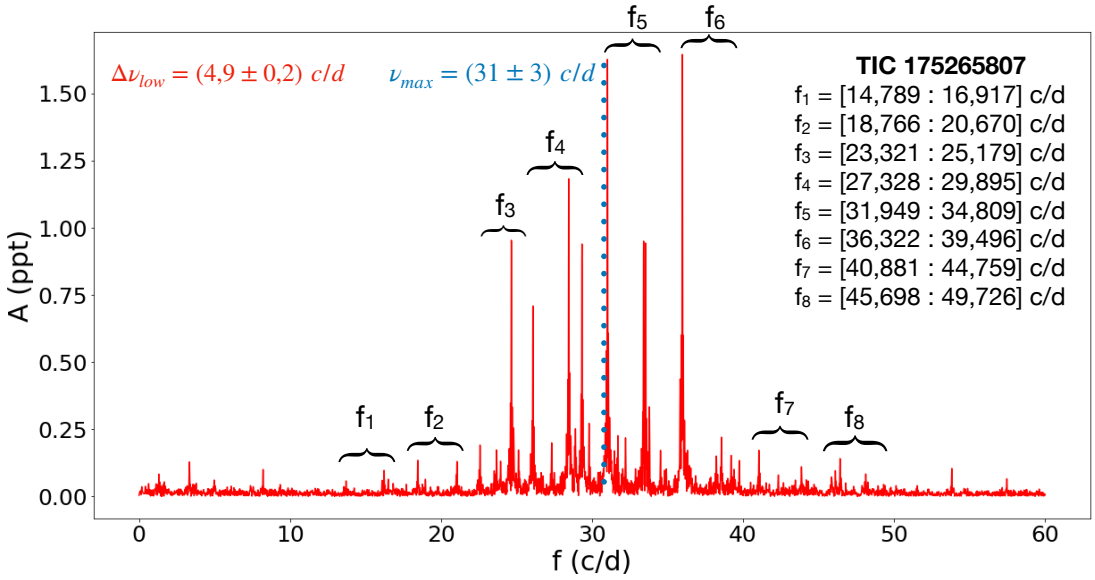

Fig. C.4: The same as Fig. 4 for TIC 175265807

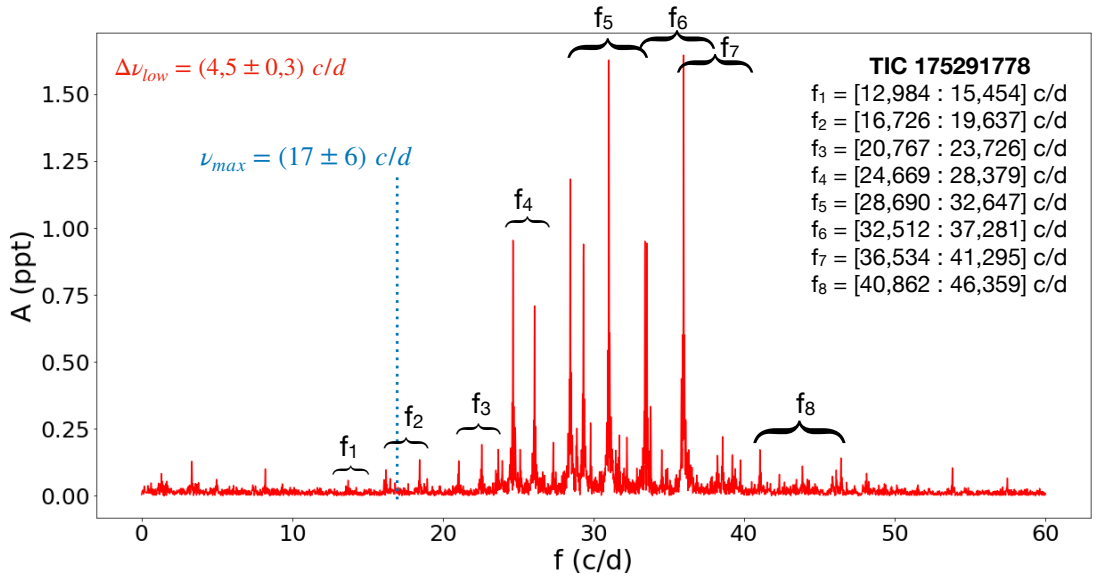

Fig. C.5: The same as Fig. 4 for TIC 175291778

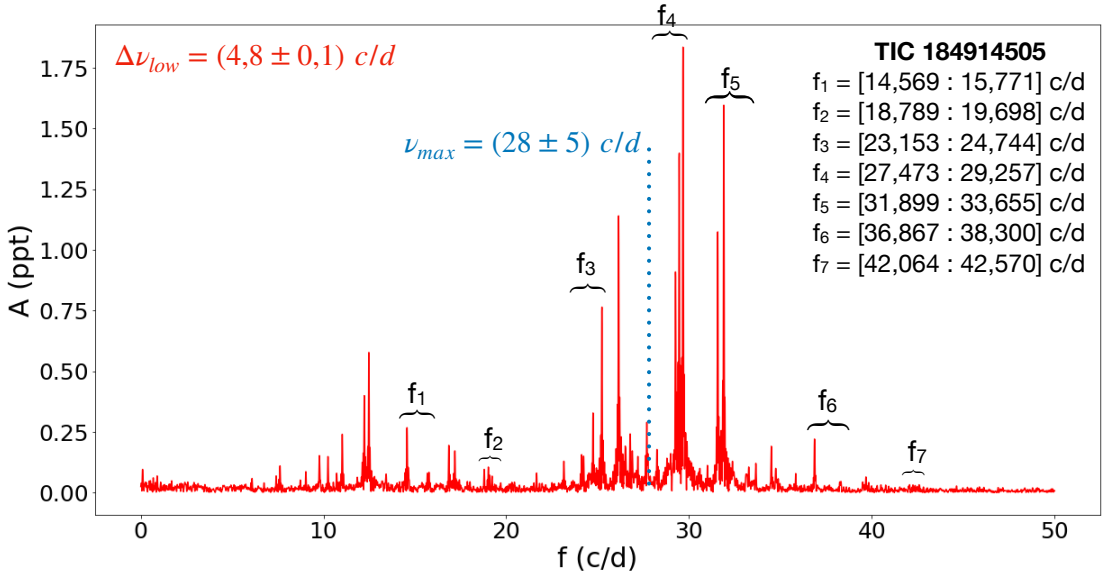

Fig. C.6: The same as Fig. 4 for TIC 184914505

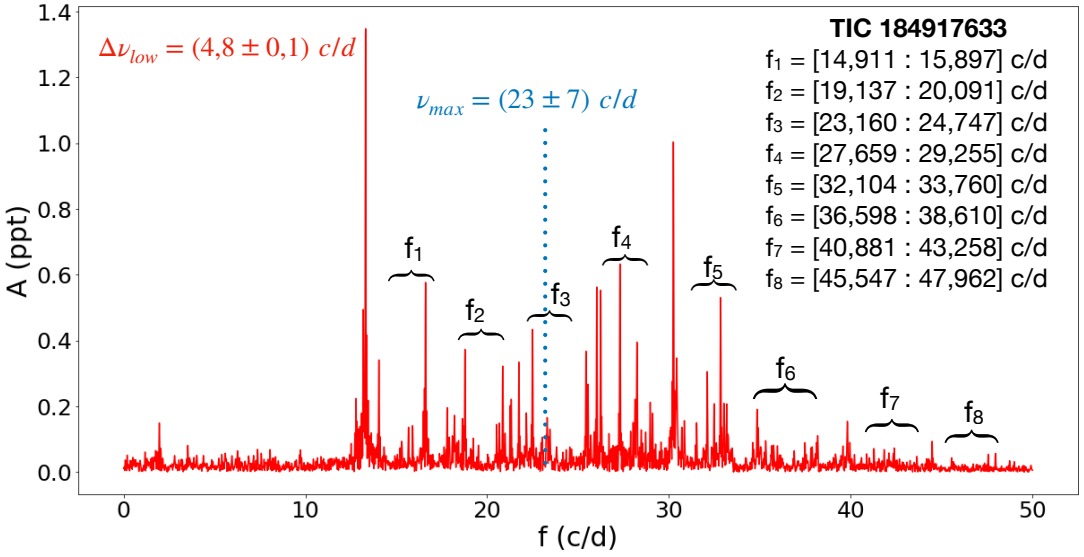

Fig. C.7: The same as Fig. 4 for TIC 184917633